

Toward Quantitative and Operator-independent Quasi-static Ultrasound Elastography: An Ex Vivo Feasibility Study

Sathiyamoorthy Selladurai¹, Abhilash Verma¹,
and Arun K. Thittai¹ 

Ultrasonic Imaging
1–12
© The Author(s) 2020
Article reuse guidelines:
sagepub.com/journals-permissions
DOI: 10.1177/0161734620921532
journals.sagepub.com/home/ux


Abstract

It is known that the elasticity of liver reduces progressively in the case of diffuse liver disease. Currently, the diagnosis of diffuse liver disease requires a biopsy, which is an invasive procedure. In this paper, we evaluate and report a noninvasive method that can be used to quantify liver stiffness using quasi-static ultrasound elastography approach. Quasi-static elastography is popular in clinical applications where the qualitative assessment of relative tissue stiffness is enough, whereas its potential is relatively underutilized in liver imaging due to lack of local stiffness contrast in the case of diffuse liver disease. Recently, we demonstrated an approach of using a calibrated reference layer to produce quantitative modulus elastograms of the target tissue in simulations and phantom experiments. In a separate work, we reported the development of a compact handheld device to reduce inter- and intraoperator variability in freehand elastography. In this work, we have integrated the reference layer with a handheld controlled compression device and evaluate it for quantitative liver stiffness imaging application. The performance of this technique was assessed on ex vivo goat liver samples. The Young's modulus values obtained from indentation measurements of liver samples acted as the ground truth for comparison. The results from this work demonstrate that by combining the handheld device along with reference layer, the estimated Young's modulus value approaches the ground truth with less error compared with that obtained using freehand compression (8% vs. 15%). The results suggest that the intra- and interoperator reproducibility of the liver elasticity also improved when using the handheld device. Elastography with a handheld compression device and reference layer is a reliable and simple technique to provide a quantitative measure of elasticity.

Keywords

compression, handheld device, liver disease, quantitative, reference layer, strain ratio, operator independent, ultrasound elastography

Introduction

Chronic liver disease results in fibrosis that may lead to cirrhosis. Especially, the prevalence of nonalcoholic fatty liver disease (NAFLD) is 80% to 90% in obese adults, 30% to 50% in patients with diabetes, and up to 90% in patients with hyperlipidemia.¹ The prevalence of NAFLD among children is 3% to 10%, rising to 40% to 70% among obese children.² Moreover, pediatric NAFLD increased from about 3% a decade ago to 5% today, with a male-to-female ratio of 2: 1.³ NAFLD is rapidly becoming the most common liver disease worldwide.^{4,5}

Diagnosis based on liver biopsy is still considered as one of the gold standards in determining the degree of liver fibrosis, which helps in the prognosis of the disease condition and guides treatment decisions in the case of chronic

liver disease. However, the use of liver biopsy has several limitations, such as invasiveness, physical, and mental discomfort to the patient.⁶ Some recent techniques, like transient elastography (TE) and shear wave elastography (SWE), have started to increasingly replace biopsy in most cases and are discussed in more detail in the subsequent paragraph. The different levels of fibrosis are assessed based on

¹Biomedical Ultrasound Laboratory, Biomedical Engineering Group, Department of Applied Mechanics, Indian Institute of Technology Madras, Chennai, India

Corresponding Author:

Arun K. Thittai, Biomedical Ultrasound Laboratory, Biomedical Engineering Group, Department of Applied Mechanics, Indian Institute of Technology Madras, Chennai 600036, Tamil Nadu, India.
Email: akthittai@iitm.ac.in

histological scores classified as F0 (no fibrosis), F1 (mild fibrosis), F2 (clinically significant fibrosis), F3 (severe fibrosis), and F4 (cirrhosis), as per the revised clinical practice guidelines for grading and staging of liver diseases.⁷⁻⁹

Therefore, there is an increasing need for alternative noninvasive methods to determine the grade of liver fibrosis and for frequent follow-up monitoring of liver after treatment. It is well known that liver stiffness is related to the degree of fibrosis, and palpation has been used over decades to establish a clinical diagnosis of hepatic fibrosis and cirrhosis. Early diagnosis can lead to reversing the disease condition and avoid liver transplantation. In the view of the above, there is an active research interest worldwide toward the development of noninvasive techniques for the assessment of liver diseases based on changes in liver stiffness. In this regard, ultrasound elastography seem to be one of the most promising approaches.¹⁰ Based on the excitation source, elastography techniques can be divided into two main subgroups: dynamic, which is based on dynamic force stimulus, and quasi-static strain elastography in which a compressive force is applied.^{11,12}

The most extensively used and tested method for evaluation of liver fibrosis and staging is TE. This technique, which does not produce images, consists of a mechanical vibrator that generates a low-frequency shear wave at 50 Hz in the target tissue (liver), and subsequently, pulse-echo ultrasound acquisitions are used to follow the propagation of the shear wave to measure its speed, C_s (m/s). The corresponding Young's modulus E (kPa) is computed by $E = 3\rho C_s^2$, where, ρ is the density of tissue.¹³ The disadvantage of this method is that it does not provide a B-mode image that is essential for accurate targeting, it cannot be performed on the liver with ascites, and it is not coupled with a standard ultrasound machine.¹⁴

On the other hand, SWE is a dynamic elastography method in which the elasticity is estimated based on the shear wave induced by an excitation. The excitation may be from an external vibrator or sources, such as an acoustic radiation force. Point SWE-based approaches provide the stiffness value only over a smaller region of interest (ROI), yet the clinical experiences and evidence are promising. However, this method will require a dedicated high-end scanner, which may make it expensive for routine scanning in rural, resource-poor regions within developing or underdeveloped countries.^{15,16}

In contrast, quasi-static elastography or real-time elastography (RTE) is shown to be feasible even with affordable low-cost scanners.^{17,18} This technique is predominantly popular in clinical applications where one wants to visualize regions with different relative stiffness within a soft-tissue region (e.g., solid lesion in breast), as against homogeneous targets. In the case of diffuse liver disease, where the liver gets stiffer as a whole, this technique has not been explored much, citing its qualitative nature and lack of any local contrast. However, it has several advantages: it is fast and painless, technique; Ascites is not a limiting factor; it can be

incorporated within conventional ultrasound diagnostic imaging scanner. It allows the combination of examination such as elastography assessment of the liver fibrosis and/or tumor after the morphological ultrasound examination of the liver (to investigate for signs of cirrhosis, portal hypertension, and to identify focal lesions). Because of the many listed advantages of this method, several efforts are being taken to make quasi-static elastography a quantitative one.

Chen et al.¹⁹ demonstrated the feasibility of estimating perineal body tissue properties in vivo in nulliparous women by using quantitative elastography and an artificial reference material. Yamamoto et al.²⁰ explored quantitative elastography for measuring the degeneration of Achilles tendon using a built-in reference layer and strain ratio metric for quantitative measurements. Hee et al.²¹ explored the feasibility of quantitative sonoelastography of the uterine cervix by using laboratory built reference material. However, in all of these studies, the challenge due to interoperator variability in compression in freehand elastography method was not addressed. Furthermore, contrast-transfer efficiency (CTE) was not incorporated while calculating Young's modulus from strain ratio. It is important to incorporate the CTE, especially for liver, as there appears to be a modulus range scale that is correlated to the disease stage, and therefore, requires more accuracy.¹⁴

In the work reported in this paper, we attempt to overcome the twin problems of quasi-static elastography (i.e., qualitative measurement and challenge of interoperator variability in freehand elastography compression method) by integrating a reference layer within a handheld controlled compression device. Recently, we demonstrated a method to quantitatively measure the unknown modulus of the examined homogenous tissue-mimicking phantom by using a reference layer with known stiffness, interpositioned between the transducer and the tissue-mimicking phantom surface.^{22,23} However, these used a benchtop three-dimensional (3D) motion controller setup to provide elastographic compression. In a separate study, the development of a compact handheld compression device for use in RTE was reported.^{24,25} In this work, a combination of the two separate developments to estimate Young's modulus of ex vivo goat liver samples is investigated. Furthermore, we also investigated the intra- and interoperator reproducibility of the elasticity measurements obtained by the use of the handheld compression device and compared it against the freehand elastography approach. The work reported in this paper and the associated findings on ex vivo liver samples is a necessary and significant prelude to translating the concept to investigate its utility in a clinical setting.

Materials and Methods

Ex Vivo Liver-embedded Phantom

Three freshly excised goat livers were acquired from a local butcher shop. Agar (3% by weight) and gelatin (5% by

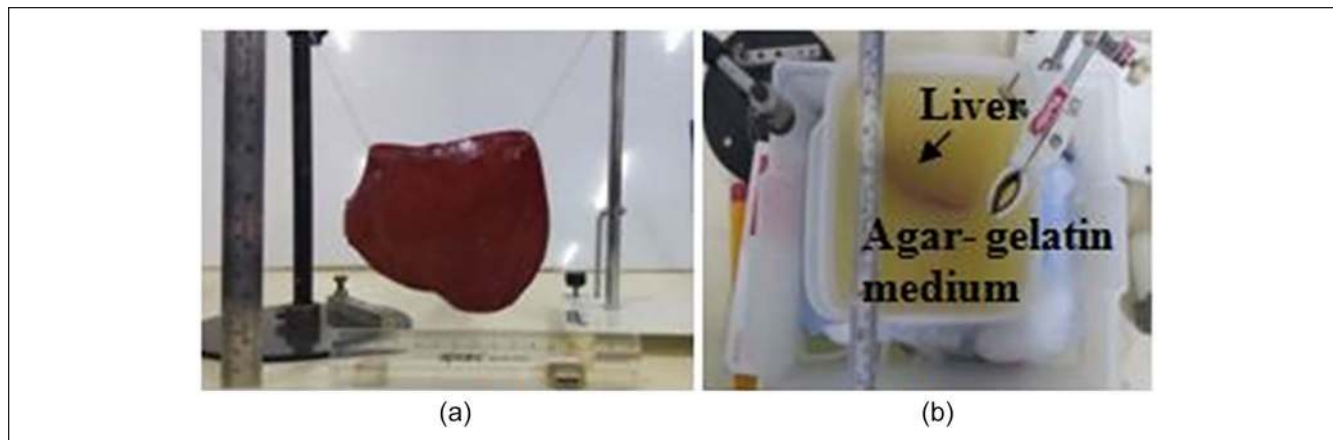


Figure 1. Photos showing (a) ex vivo liver suspended by stitching thread and held in place before agar–gelatin phantom solution is poured to surround it and (b) top view of the final liver-embedded Phantom.

weight) were mixed with de-ionized water and heated to 80°C and stirred with a magnetic mixer until the temperature came down to about 30°C. The mixture was then poured into a mold that contained the liver sample, which was suspended by using a stitching thread, as shown in Figure 1. Thus, the agar–gelatin solution acts as surrounding tissue-mimicking material for liver. The phantom was of the dimension 10 × 16 × 16 (height × length × width, in cm). The liver-embedded phantom in mold was then placed in the refrigerator at 5°C for 8 hours before any mechanical and elastography testing was done on it. In the same manner, a total of three ex vivo liver-embedded phantoms were prepared.

Reference Layer

A commercially available 2 (height) × 9 cm (diameter) aqueous, flexible, disposable ultrasound standoff layer (Aquaflex[®], Parker Laboratories, New Jersey) was used as a reference layer. Its modulus value was determined from indentation test using Universal Testing Machine (UTM; Jinan TE, China), which is explained in detail in the upcoming section “Measurement of Young’s Modulus Using UTM.”

Handheld Controlled Compression Device

A snapshot of the handheld device setup is shown in Figure 2. The controlled compression is achieved by programming the movement of the external compressor attachment, instead of the transducer itself; therefore, the device can be attached to several different ultrasound transducers, irrespective of their size and weight. A spindle geared motor, a position sensor, and a controller manufactured by Maxon Motor AG (Sachseln, Switzerland) were used in the device to move the compressor uniaxially. This device is integrated with an L14-5/38 transducer (Analogic, Peabody, Massachusetts) operating at frequency of 6.6 MHz (corresponding to “penetration mode” in SonixTouch Q+[®] scanner), which was used for

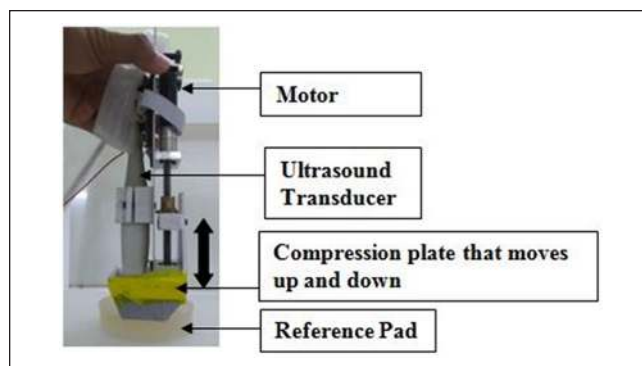


Figure 2. Photo of the handheld controlled compression setup (side view) along with reference pad.

radio-frequency (RF) data acquisition. The acquired RF data were sampled at 40 MHz sampling frequency. The device was set to provide axial compression and relaxation of 2% at 1 Hz on the ex vivo liver-embedded phantom for five cycles. A description of the device development and performance can be found in reference.^{24,25} Note that the device is designed such that the compressor plate is the one that is moving and not the transducer. Therefore, we could swap out the transducer probe and this may take additional time. However, the actual scanning time of the proposed method is going to be the same compared with that of conventional scanning.

Data Acquisition

The experimental data acquisition was performed using a SonixTouch Q+[®] scanner. The elastograms were collected using a single focus at a depth of 40 mm from the surface of the transducer. The elastography experiments were performed, having the reference layer in between the transducer and the agar–gelatin background containing the liver sample. The compression–relaxation cycles were applied with

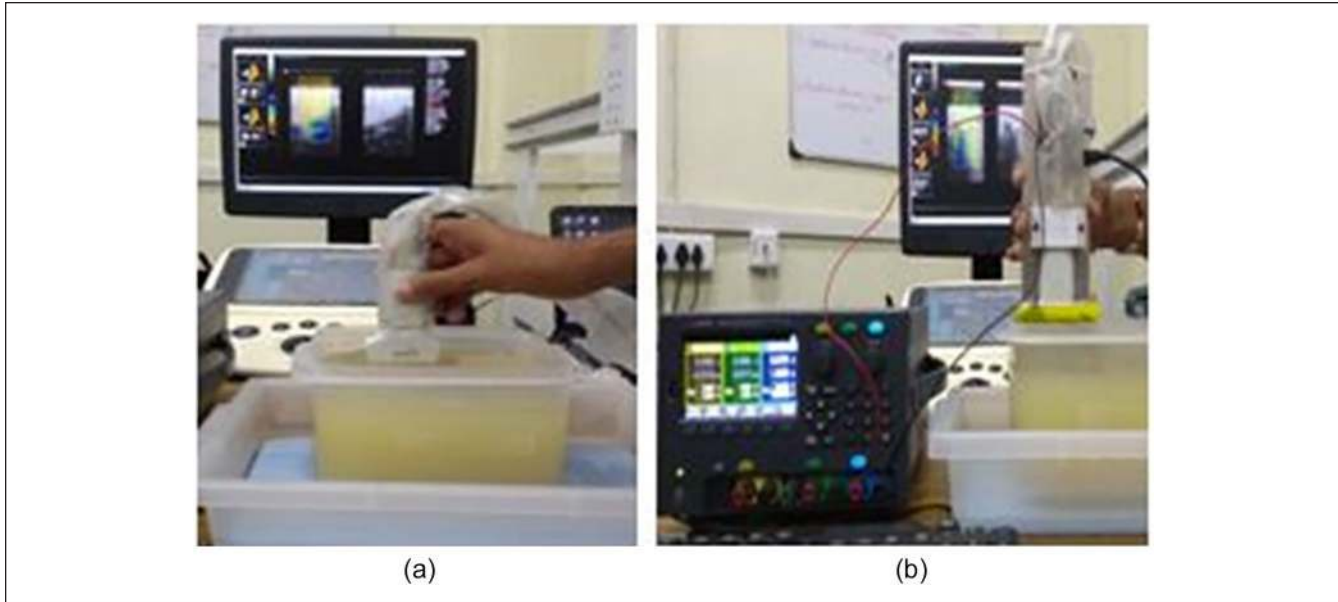


Figure 3. A photograph of the actual elastography data acquisition set up using Sonix Touch Q+ ultrasound scanner during (a) freehand compression and (b) handheld device compression.

freehand, and also automatically with the handheld compression device, and data were acquired for five seconds (50 frames/s). For each acquisition, elastograms were stored as cine loops in the scanner memory.

Five different operators (excluding the authors) were instructed to perform elastography experiments using the handheld compression device and freehand (i.e., using transducer only) with the calibrated reference layer placed on the top of the phantom (as shown in the Figure 3). In the case of freehand compression, the quality indicator on the screen of the scanner provided a visual feedback to the operators for maintaining a suitable range and uniformity of compression. Vascular structures in the liver were avoided during the scanning procedure to make measurements reliable. The above experiment was repeated on the same liver sample for five times, but at different elevational planes separated by 5 mm, to obtain independent realizations. The same experimental procedure was followed for imaging all the three different liver samples.

Frame Selection Algorithm

From the stored elastography cine loop, good quality frame(s) was selected by a frame selection algorithm²⁶ that automatically selects a few representative frames for further analysis. Previously, the performance of this automated algorithm was reported by Chintada et al.,²⁷ where automated representative frame selections were compared against those selected by trained radiologists and found to reduce interobserver variations that arise at least partly because of the differences in the selection of representative frames from a cine loop. Linear elasticity is an implicit

assumption in the frame selection algorithm. In fact, frame selection algorithm may not be affected as long as piecewise linearity is there, which may be the case at common frame rates practiced (>10 frames per seconds).²⁶

Strain Ratio Calculation

From the selected representative elastogram frames, the strain values from the reference layer and liver region were extracted over the ROI using the built-in software of the scanner. The strain distribution within an ROI is often illustrated by a color map, where large strain (lower stiffness) is indicated in blue and small strain (higher stiffness) in red. The strain ratio between two ROIs was then calculated.

When assessing the strain by elastography, the distance between the ROI and the transducer was taken into account,²⁸⁻³⁰ as the tissue closest to the transducer receives more compression than the tissues further away. The influence of choosing the position of the ROIs in elastography is reported by Nakayama et al.³¹ The Young's moduli obtained at lateral border of the elastography image are not reliable. The strain ratio measurements were therefore obtained relatively close to the center line of the image. Guided by the literature, the distance between the ROI and the reference layer was kept as constant as possible for all measurements for comparison.

Young's Modulus Estimate from Strain Ratio

The unknown modulus of the liver is estimated after first obtaining the phantom-to-reference layer modulus contrast using the following relationship^{32,33}:

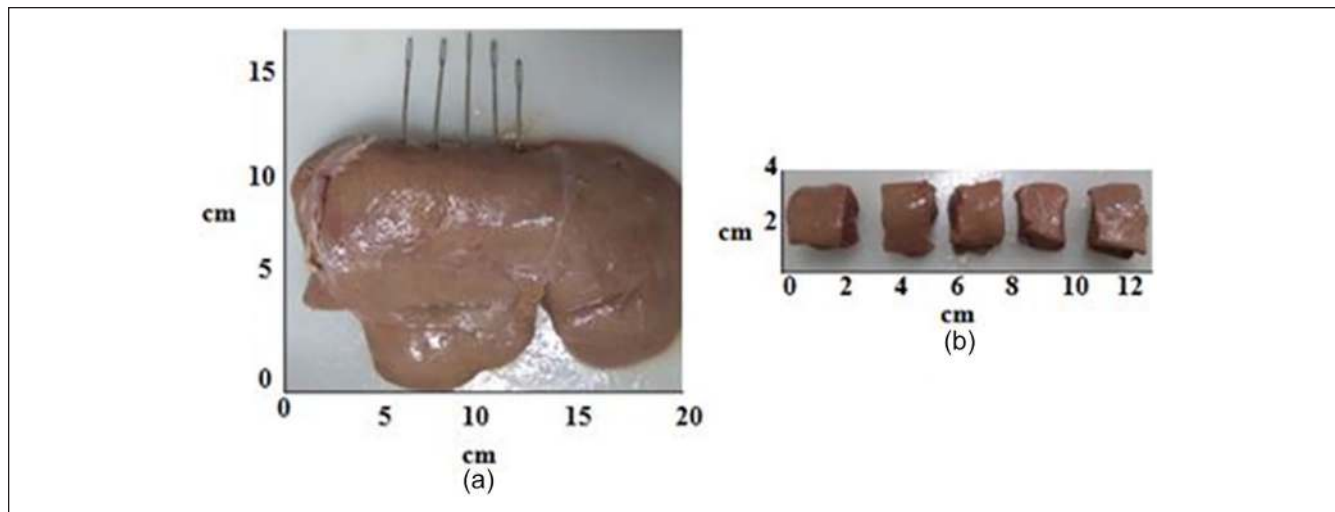


Figure 4. Image showing (a) the liver sample with needle insertions, which acts as a marker to identify the corresponding imaging planes and (b) the samples cut out from the liver for UTM testing. UTM = Universal Testing Machine.

$$C_m = |2C_s - 1|, \quad (1)$$

where C_s is the strain contrast and C_m is the corresponding modulus contrast. Later, using the known modulus value of the reference material (obtained from indentation testing described in the “Measurement of Young’s Modulus Using UTM” section), along with the estimated modulus contrast, we can obtain the unknown target modulus using Equation (2):

$$\frac{M_1(\text{unknown})}{M_2(\text{known})} = C_m, \quad (2)$$

where M_1 = modulus of the liver (unknown), M_2 = modulus of the reference layer.

Measurement of Young’s Modulus Using UTM

The embedded liver sample was taken out by removing the background agar–gelatin material without disturbing the needles that were placed as markers for identifying the imaging planes, as shown in Figure 4(a). The liver samples were cut into required dimensions as shown in Figure 4(b) using a surgical knife along the identified imaging planes. Samples were cut such that their height is less than twice their diameter to avoid the buckling effect.^{34,35}

Liver samples were tested by a computer-controlled electro-mechanical UTM (Jinan TE, China). The 5 kN machine is equipped with an extensometer with 50 mm gauge length. The load cell measures the test load, and an elastometer measured the deformation of the specimen. Compression test was performed under displacement controlled mode with a strain rate of 1 mm/min up to a maximum of 15% strain. All samples were preconditioned for five seconds and preloaded

to 1% of strain (1 mm). This experiment was repeated on five different samples from the same liver to measure the modulus value. Young’s modulus was calculated from the slope of the linear portion of the loading curve using the least square fit. The slope was considered to be linear up to a maximum of 5% strain.³⁴ The same procedure was followed for calculating the modulus value of the reference layer.

Figure 5 shows a schematic of the process for comparing Young’s modulus measurements obtained from Quasi-static ultrasound elastography (freehand and device compression), along with the results obtained from UTM testing.

Results

Ex Vivo Experiments

Figure 6 shows the stress–strain plot obtained from UTM for one of the liver samples. The modulus values of different samples calculated from the slope of the stress–strain curve are reported later in Table 1.

Figure 7 compares the quality of the frames in the cine loop, which were acquired using freehand compression and the handheld device, respectively, for the same liver-embedded phantom. Here, the quality of the frames was determined by the frame selection algorithm that was reported in previous section. Only those frames that passed the threshold for sufficient compression (0.5%–2%), correlation coefficient (0.8–1), and tilt angle (0°–10°) were considered to indicate good quality and selected by the algorithm. The thresholds were taken to be the same as those reported earlier.^{27,36} It can be inferred from Figure 7 that more number of good quality elastograms are obtained in the data acquired by handheld device compression compared with that of freehand elastography.

Figure 8 shows an example of the axial displacement map and corresponding strain elastogram selected by the frame

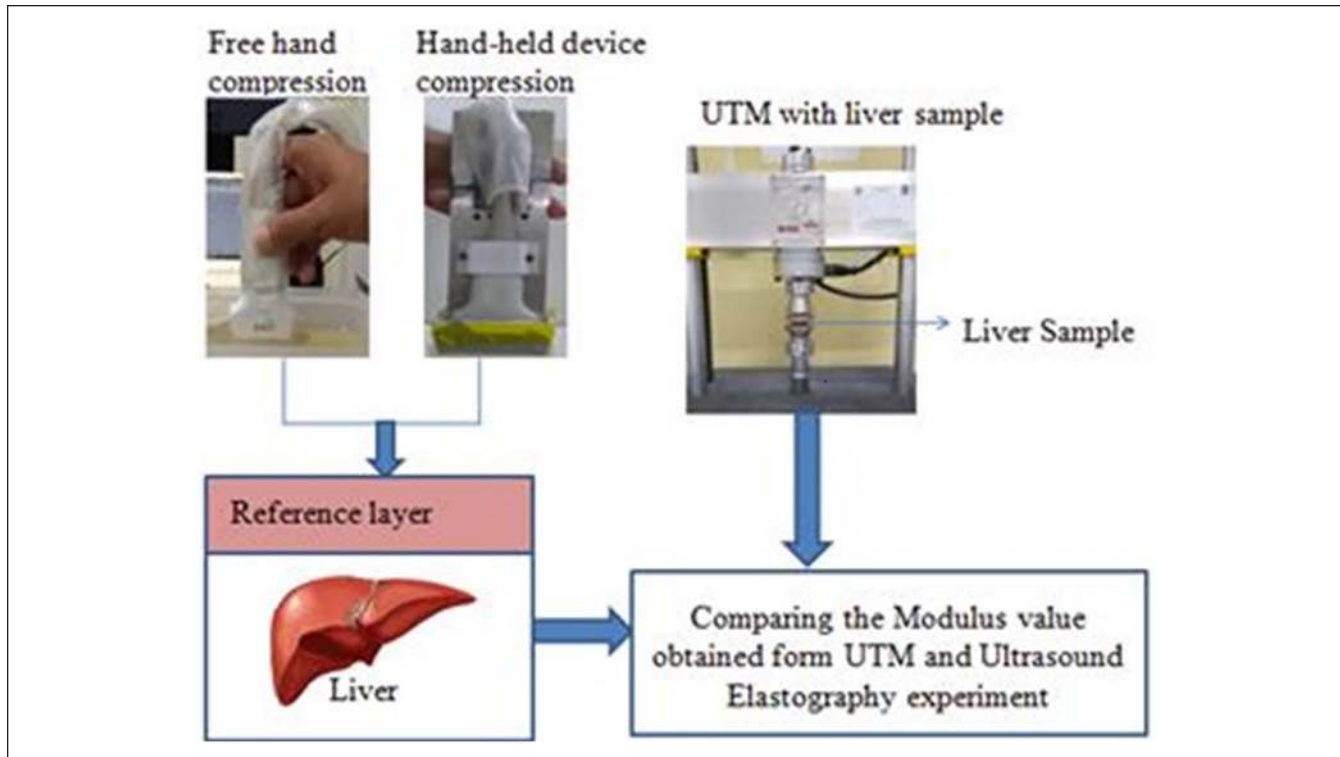


Figure 5. A schematic representation of the process for comparing the measurements obtained from quasi-static elastography (freehand and handheld device compression) integrated with the reference layer to that of UTM measurements. UTM = Universal Testing Machine.

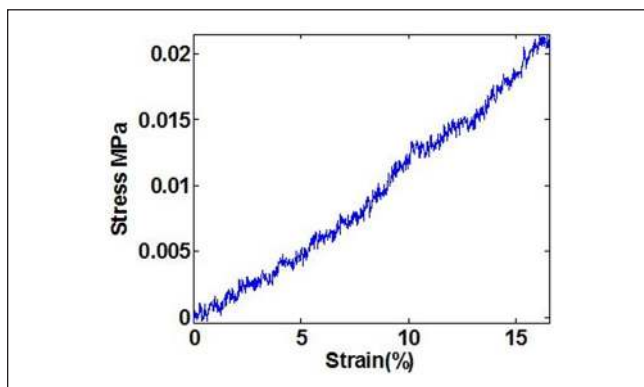


Figure 6. The plot of the stress–strain loading curve for one liver sample. The linear region is fixed at the initial portion (5% of strain), and Young's modulus was calculated as the slope of this linear portion using the least square fit.

selection algorithm. It can be noticed that the axial displacement contours are parallel, especially, at shallow depths, indicating very little tilt during compression as would be expected for the case of uniform applied compression.

Figure 9 shows the screenshot of B-mode image and strain elastogram of one imaging plane obtained from freehand and handheld compression device, respectively. The unknown modulus value of the liver was estimated from the

strain contrast values taken from the ROI, indicated by red box, and using Equation (2). The obtained modulus values were compared with the values obtained from UTM experiments and reported in Figures 10 to 12.

Table 1 shows Young's modulus value obtained from UTM (ground truth) and by ultrasound elastography with reference layer using freehand compression and handheld device compression methods for the three different embedded liver samples. The mean and standard deviation values computed over five independent realizations of elastography and UTM experiments are reported.

Figures 10 to 12 show the corresponding bar plot of values tabulated in Table 1 for the different samples, liver 1, 2, and 3. It can be observed that the intra- and interoperator reproducibility of the liver elasticity also improved when using the handheld device. It can be inferred from this result that by combining the handheld device along with reference layer, the estimated Young's modulus value approaches very close to the ground truth (within 8% error) compared with that of results obtained using freehand compression (within 15% error with respect to ground truth).

Discussion and Conclusion

Quasi-static elastography using external reference layer is a reliable and simple technique for the assessment of liver

Table 1. The Mean and Standard Deviation Values of the Young's Modulus of Liver Obtained in Experiments.

Liver Sample	Type of Compression Used	Liver 1 Liver: 12 ± 5.12 (Ground Truth)	Liver 2 Liver: 14 ± 4.45 (Ground Truth)	Liver 3 Liver: 10 ± 4.27 (Ground Truth)
Operator 1	A	17 ± 6.28	18 ± 5.92	16 ± 6.17
	B	13 ± 2.33	13 ± 1.68	9 ± 2.83
Operator 2	A	19 ± 4.23	20 ± 3.83	17 ± 4.79
	B	14 ± 2.14	14 ± 2.75	12 ± 1.84
Operator 3	A	18 ± 5.49	19 ± 4.90	15 ± 5.63
	B	11 ± 1.50	12.5 ± 2.14	11 ± 3.26
Operator 4	A	16.5 ± 4.33	17 ± 3.26	15.5 ± 4.28
	B	13 ± 2.75	13 ± 2.17	12.5 ± 2.73
Operator 5	A	18 ± 5.81	18 ± 4.96	18 ± 5.21
	B	13 ± 2.57	12 ± 1.75	11 ± 2.64

The Young's modulus value obtained from UTM for reference layer: 20 ± 1.7 (which is used for calculating unknown modulus). A = estimated modulus value from freehand compression (kPa). B = estimated modulus value from handheld compression device (kPa). UTM = Universal Testing Machine.

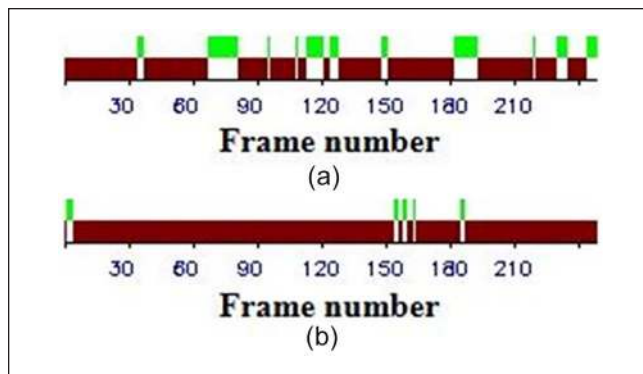


Figure 7. Total frames in the cine loop acquired using (a) freehand compression and (b) handheld device compression. Only those frames that passed the threshold for sufficient compression, correlation coefficient, and tilt angle were color-coded as “green” to indicate good quality.

elasticity. The use of external reference layer integrated with a handheld compression device can provide a quantitative measure of liver elasticity. The results suggest that the unknown tissue stiffness (goat liver) was estimated within an error of 8% in experiments. It is also observed from the results shown in Figures 10 to 12 and Table 1 that the proposed method has minimal inter- and intraoperator variability.

The handheld device essentially takes advantage of two aspects: (a) the larger footprint of the compressor plate compared with the transducer footprint and (b) controlled compression. The effect of compressor plate size used for providing compression in freehand quasi-static elastography has been reported extensively in the literature.^{37,38} A narrow compressor generates strain that is concentrated below the compressor and decays rapidly with depth. A compressor of lateral and elevational width equal to or greater than the lateral extent of the region imaged is needed to create the most

homogeneous strain distribution and to maximize the depth of stress penetration.³⁹⁻⁴¹ Along with advantage of larger compressor plate footprint, the rate and amount of compression can be controlled by using the proposed device, which helps in reducing the interoperator variability in freehand elastography. Note that the compressor plate dimension can be reduced and refined further based on in vivo clinical translation demands.

Regarding the choice of material for the reference layer, we initially tried using phantoms made of agar/gelatin mixtures. However, the stability and shelf-life of the in-house manufactured pad were found to be very limited. Therefore, a commercially available standoff pad was tested for its potential to serve as the reference material, which was also suggested recently by Yamamoto et al.²⁰ The results suggest that their Young's modulus value changed very little over the four-month period of testing. Nevertheless, one has to take care that the standoff pad is stored and maintained properly. If the mechanical properties of the pad change, it will greatly affect our results because only the calibrated modulus value of the reference pad is considered for the estimation of the unknown modulus value.

Although the model proposed in this paper does not exactly reflect the complex in vivo imaging conditions, it is an initial attempt to demonstrate the development on some real tissue instead of just tissue-mimicking phantoms. Thus, the experiments on goat liver samples embedded in agar-gelatin mixtures were meant to be part of preliminary investigation and on the aspect of having rib cage and other tissue types in between are left for future studies. The addition of subcutaneous fat and ribs could dampen the stress and may contribute to some inaccuracies. Nevertheless, some suggestions from literature^{42,43} that can be used to improve the quality of acquisition when translating to in vivo conditions where rib cage and other tissue types may be present are listed below:

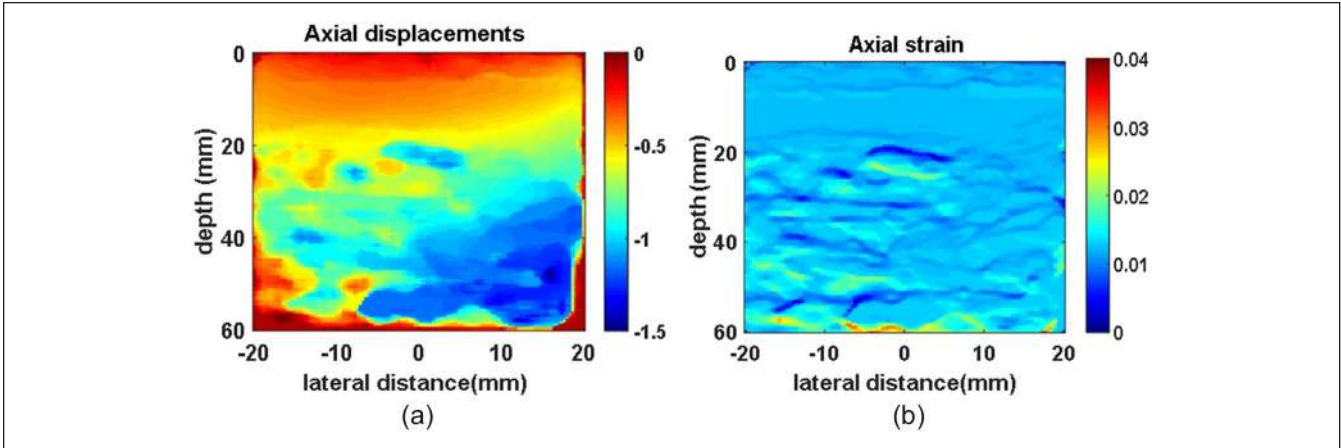


Figure 8. An example frame of (a) axial displacement map and (b) corresponding axial strain elastogram, selected by the frame selection algorithm is shown. Notice that the axial displacement contours are mostly parallel to each other as it would be for a uniform compression. The frame selection algorithm uses an estimate of the tilt angle from the axial displacement and frame-average axial strain as parameters to decide on amount and tilt in compression.

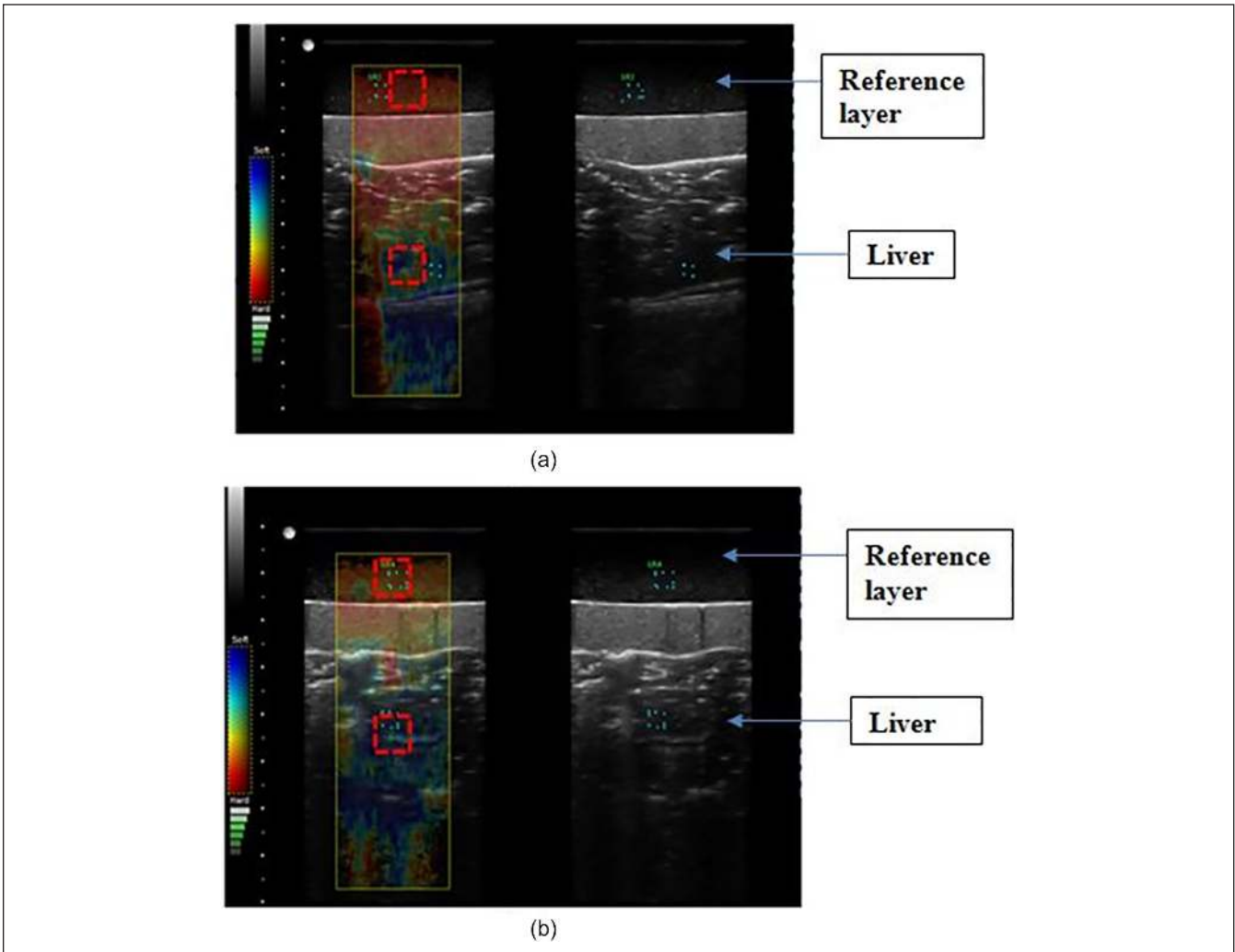


Figure 9. Screenshot of elastograms from Sonix Touch Q+ ultrasound scanner obtained by (a) freehand compression and (b) handheld device compression. The red box on the image represents the ROI from which the strain ratios were computed. ROI = region of interest.

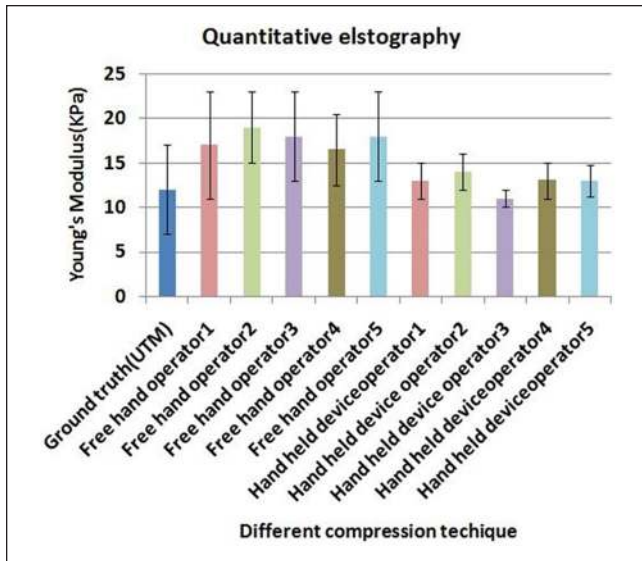


Figure 10. The mean and standard deviation values of liver 1 Young's Modulus values obtained from UTM, freehand compression, and handheld device compression of the five operators for strain ratio calculated from Scanner software. UTM = Universal Testing Machine.

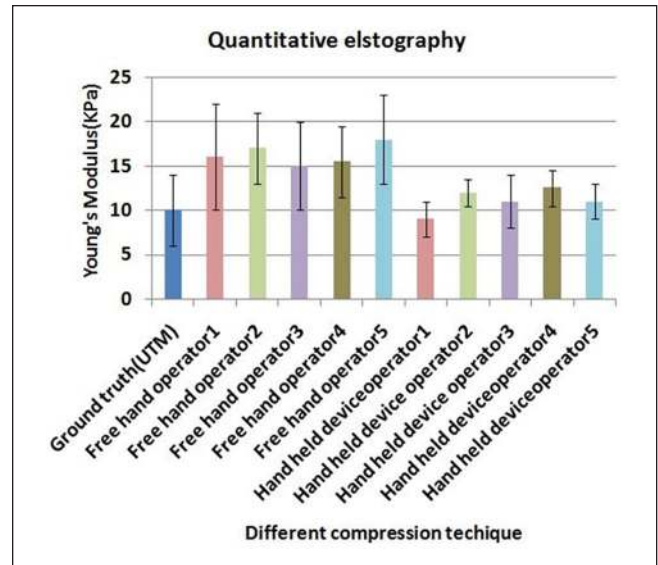


Figure 12. The mean and standard deviation values of liver 3 Young's Modulus values obtained from UTM, freehand compression, and handheld device compression of the five operators for strain ratio calculated from Scanner software. UTM = Universal Testing Machine.

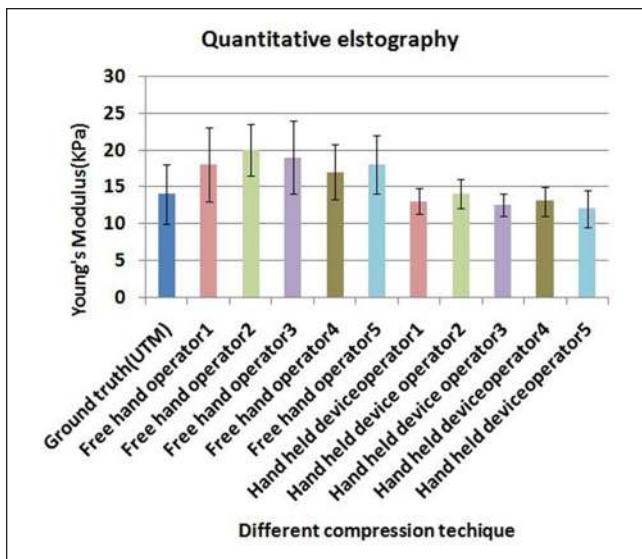


Figure 11. The mean and standard deviation values of liver 2 Young's Modulus values obtained from UTM, freehand compression, and handheld device compression of the five operators for strain ratio calculated from Scanner software. UTM = Universal Testing Machine.

- image the right liver lobe through an intercostal space (eighth or ninth intercostal space can be selected as the scanning site) with the patient supine and the right arm elevated to widen the intercostal space;
- the handheld controlled compression device used here needs to impart repeated compression-relaxation to the tissue to induce the necessary strain;

- selecting an ROI that is free from interfering structures and artifacts;
- have the patient perform a short breath hold to ensure that strain elastography (SE) images are displayed consistently.

all the other factors listed in Barr et al.,⁴⁴ will need to be evaluated.

Furthermore, the focus of the paper was to investigate and report on an approach using reference layer and controlled compression setup to make quasi-static elastography a quantitative technique and reduce the inter-/intraoperator variability. Therefore, the performance of the proposed method was not tested for varied range of liver stiffness or other abnormal conditions like, for example, steatosis. However, in literature, it is suggested that ultrasonic strain elastography can be used for quantitative (i.e., strain ratio) assessment of the severity of fatty liver.^{45,46} Proposed method is an improvised extension of the strain elastography, and therefore, it is reasonable to hypothesize that the proposed method will also work equally well at different stiffness value and it may also be useful to stage steatosis condition of liver.

Furthermore, it should be noted that in the proposed approach, strain contrast is calculated first, followed by calculation of modulus contrast using CTE (i.e., Equation (1)). Finally, the quantitative Young's modulus value is estimated using the known modulus values of the reference layer and the calculated modulus contrast. Therefore, it is fair to anticipate that the strain distribution may change depending on the different type of tissues along the compression path. Having slip boundary condition at interfaces could be the most

challenging of them. However, prior work by our group has demonstrated that even in the more complex case of having stiff or soft inclusion with slip boundary condition, the error in CTE can be made less than 5% by carefully choosing the ROI to calculate the strain ratio.⁴⁷ In comparison with having an inhomogeneity with slip boundary condition, the estimation in liver target should be less error prone due to it being more homogeneous compared with a lesion in a background case. Also, Equation (1) assumes linear elasticity,^{32,33} which is a fundamental aspect in quasi-static elastography and may be acceptable as long as the compression is within a small strain range. This condition will probably be satisfied because the image quality will also be good only in the small strain range (~0.5%-2%) dictated by the strain filter concept. Nevertheless, the applicability of Equation (1) in complex scenarios will have to be paid more attention in future while clinically translating this approach.

Other quantitative methods include TE and SWE, which are available already in clinical practice. However, there seems to be an issue with measurement variation from scanner to scanner that is still being addressed for liver imaging.^{10,48} Furthermore, these methods need a dedicated high-end scanner system.^{11,49} One of the major advantages of the proposed approach is that it can be easily used with a standard ultrasound scanner having elastography software and a calibrated reference layer that is commercially available. Furthermore, we standardized the scanning procedure for quantitative quasi-static elastography by providing controlled and precise compression using handheld controlled compression device. It would be interesting to compare the proposed methodology with TE and SWE (state of the art) through an in vivo clinical study, which is left for future work.

There are several methods reported in the literature that seeks to estimate the modulus image from displacement and strain data from axial and lateral directions using inverse reconstruction techniques.⁵⁰ It is possible that some of the simple inverse reconstruction methods that are real time can be adopted for the case considered. In general, the accuracy, robustness, and speed of inverse reconstruction improve with better quality input estimates of axial and lateral displacement data.⁵⁰ Recently, there have been many methods proposed to obtain better quality lateral displacement estimates in elastography.^{18,51-53} We are currently investigating on combining the reference layer methodology and inverse reconstruction approach having access to better quality lateral displacement estimates, and compare it with the simple approach proposed here.

Acknowledgments

The authors thank the Ministry of Human Resource Development, Government of India, for awarding Half time Teaching/Research Assistantship (HTRA) scholarship to the PhD scholar through IIT Madras. The authors would like to thank Dr. A. Arockiarajan and Dr. Pijush Ghosh of IIT Madras for providing access to the Universal Testing Machine (UTM) for experiments.

Declaration of Conflicting Interests

The author(s) declared no potential conflicts of interest with respect to the research, authorship, and/or publication of this article.

Funding

The author(s) disclosed receipt of the following financial support for the research, authorship, and/or publication of this article: This work was supported by a seed grant from the Indian Institute of Technology Madras to A.K.T.

ORCID iD

Arun K. Thittai  <https://orcid.org/0000-0002-0061-661X>

References

1. Bellentani S. The epidemiology of non-alcoholic fatty liver disease. *Liver International*. 2017;37:81-4.
2. Le MH, Devaki P, Ha NB, Jun DW, Te HS, Cheung RC, et al. Prevalence of non-alcoholic fatty liver disease and risk factors for advanced fibrosis and mortality in the United States. *PLoS ONE*. 2017;12(3):e0173499.
3. Alkhatir SA. Paediatric non-alcoholic fatty liver disease: an overview. *Obes Rev*. 2015;16:393-405.
4. Perumpail BJ, Khan MA, Yoo ER, Cholankeri G, Kim D, Ahmed A. Clinical epidemiology and disease burden of non-alcoholic fatty liver disease. *World J Gastroenterol*. 2017;23(47):8263-76.
5. Cai J, Zhang XJ, Li H. Progress and challenges in the prevention and control of nonalcoholic fatty liver disease. *Med Res Rev*. 2018;39:328-48.
6. Jeong WK, Lim HK, Lee H-K, Jo JM, Kim Y. Principles and clinical application of ultrasound elastography for diffuse liver disease. *Ultrasonography*. 2014;33(3):149-60.
7. Goodman ZD. Grading and staging systems for inflammation and fibrosis in chronic liver diseases. *J Hepatol*. 2007;47(4):598-607.
8. Castera L, Bedossa P. How to assess liver fibrosis in chronic hepatitis C: serum markers or transient elastography vs. liver biopsy? *Liver International*. 2011;31:13-7.
9. Suk KT, Baik SK, Yoon JH, Cheong JY, Paik YH, Lee CH, et al. Revision and update on clinical practice guideline for liver cirrhosis. *Korean J Hepatol*. 2012;18(1):1-21.
10. Colombo S, Buonocore M, Del Poggio A, Jamoletti C, Elia S, Mattiello M, et al. Head-to-head comparison of transient elastography (TE), real-time tissue elastography (RTE), and acoustic radiation force impulse (ARFI) imaging in the diagnosis of liver fibrosis. *J Gastroenterol*. 2012;47(4):461-9.
11. Varghese T. Quasi-static ultrasound elastography. *Ultrasound Clin*. 2009;4:323-38.
12. Dewall RJ. Ultrasound elastography: principles, techniques, and clinical applications. *Crit Rev Biomed Eng*. 2013;41(1):1-19.
13. Sandrin L, Fourquet B, Hasquenoph J-M, Yon S, Fournier C, Mal F, et al. Transient elastography: a new noninvasive method for assessment of hepatic fibrosis. *Ultrasound Med Biol*. 2003;29(12):1705-13.
14. Frulio N, Trillaud H. Ultrasound elastography in liver. *Diagn Interv Imaging*. 2013;94:515-34.
15. Kishimoto R, Suga M, Koyama A, Omatsu T, Tachibana Y, Ebner DK, et al. Measuring shear-wave speed with point

- shear-wave elastography and MR elastography: a phantom study. *BMJ Open*. 2017;7(1):e013925.
16. Bercoff J, Tanter M, Fink M. Supersonic shear imaging: a new technique for soft tissue elasticity mapping. *IEEE Trans Ultrason Ferroelectr Freq Control*. 2004;51:396-409.
 17. Redhu N, Rastogi D, Yadav A, Hariprasad S, Jigar Z, Tripathi S, et al. Ultrasound elastography—review. *Curr Med Res Pract*. 2015;5:67-71.
 18. Lokesh B, Thittai AK. Diverging beam with synthetic aperture technique for rotation elastography: preliminary experimental results. *Phys Med Biol*. 2018;63(20):20LT01.
 19. Chen L, Low LK, DeLancey JO, Ashton-Miller JA. In vivo estimation of perineal body properties using ultrasound quasistatic elastography in nulliparous women. *J Biomech*. 2015;48(9):1575-9.
 20. Yamamoto Y, Yamaguchi S, Sasho T, Fukawa T, Akatsu Y, Nagashima K, et al. Quantitative ultrasound elastography with an acoustic coupler for Achilles tendon elasticity: measurement repeatability and normative values. *J Ultrasound Med*. 2016;35(1):159-66.
 21. Hee L, Sandager P, Petersen O, Uldbjerg N. Quantitative sonoelastography of the uterine cervix by interposition of a synthetic reference material. *Acta Obstet Gynecol Scand*. 2013;92(11):1244-9.
 22. Selladurai S, Thittai AK. Quantitative quasi-static ultrasound elastography using reference layer: a preliminary assessment. In: 2018 IEEE International Ultrasonics Symposium (IUS), Kobe, Japan, 22-25 October 2018, p.1-4. IEEE.
 23. Selladurai S, Thittai AK. Towards quantitative quasi-static ultrasound elastography using a reference layer for liver imaging application: a preliminary assessment. *Ultrasonics*. 2019;93:7-17.
 24. Abhilash V, Thittai AK. Development of a compact hand-held device for use in quasi-static elastography: a preliminary study on tissue-mimicking phantom. In: 16th International Tissue Elasticity Conference, Avignon, France, 9-12 September 2018, p. 40.
 25. Abhilash V. Development of a compact hand-held device for operator-independent quasi-static elastography. Master's thesis, Indian Institute of Technology Madras, Chennai, India.
 26. Xia R, Tao G, Thittai AK. Dynamic frame pairing in real-time freehand elastography. *IEEE Trans Ultrason Ferroelectr Freq Control*. 2014;61(6):979-85.
 27. Chintada BR, Subramani AV, Raghavan B, Thittai AK. A novel elastographic frame quality indicator and its use in automatic representative-frame selection from a cine loop. *Ultrasound Med Biol*. 2017;43(1):258-72.
 28. Molina FS, Gomez LF, Florido J, Padilla MC, Nicolaidis KH. Quantification of cervical elastography: a reproducibility study. *Ultrasound Obstet Gynecol*. 2012;39(6):685-9.
 29. Hernandez-Andrade E, Hassan SS, Ahn H, Korzeniewski SJ, Yeo L, Chaiworapongsa T, et al. Evaluation of cervical stiffness during pregnancy using semiquantitative ultrasound elastography. *Ultrasound Obstet Gynecol*. 2013;41(2):152-61.
 30. Ponnekanti H, Ophir J, Cespedes I. Ultrasonic imaging of the stress distribution in elastic media due to an external compressor. *Ultrasound Med Biol*. 1994;20(1):27-33.
 31. Nakayama M, Ariji Y, Nishiyama W, Ariji E. Evaluation of the masseter muscle elasticity with the use of acoustic coupling agents as references in strain sonoelastography. *Dentomaxillofac Radiol*. 2014;44(3):20140258.
 32. Kallel F, Bertrand M, Ophir J. Fundamental limitations on the contrast-transfer efficiency in elastography: an analytic study. *Ultrasound Med Biol*. 1996;22(4):463-70.
 33. Kallel F, Pihoda CD, Ophir J. Contrast-transfer efficiency for continuously varying tissue moduli: simulation and phantom validation. *Ultrasound Med Biol*. 2001;27(8):1115-25.
 34. Manickam K, Machireddy RR, Seshadri S. Characterization of biomechanical properties of agar based tissue mimicking phantoms for ultrasound stiffness imaging techniques. *J Mech Behav Biomed Mater*. 2014;35:132-43.
 35. Manickam K, Machireddy RR, Seshadri S. Study of ultrasound stiffness imaging methods using tissue mimicking phantoms. *Ultrasonics*. 2014;54(2):621-31.
 36. Xia R, Thittai AK. Method to estimate the deviation from ideal uniaxial compression during freehand elastography. *Ultrasound Imaging*. 2015;37(1):70-82.
 37. Konofagou E, Dutta P, Ophir J, Cespedes I. Reduction of stress nonuniformities by apodization of compressor displacement in elastography. *Ultrasound Med Biol*. 1996;22(9):1229-36.
 38. Love AEIX. The stress produced in a semi-infinite solid by pressure on part of the boundary. *Philos T R Soc Lond*. 1929;228(659-669):377-420.
 39. Kolen AF. Elasticity imaging for monitoring thermal ablation therapy in liver. PhD thesis, University of London, 2003.
 40. Doyley MM, Bamber JC, Fuechsel F, Bush NL. A freehand elastographic imaging approach for clinical breast imaging: system development and performance evaluation. *Ultrasound Med Biol*. 2001;27(10):1347-57.
 41. Varghese T, Zagzebski JA, Frank G, Madsen EL. Elastographic imaging using a handheld compressor. *Ultrasound Imaging*. 2002;24(1):25-35.
 42. Dietrich CF, Bamber J, Berzigotti A, Bota S, Cantisani V, Castera L, et al. EFSUMB guidelines and recommendations on the clinical use of liver ultrasound elastography, update 2017 (long version). *Ultraschall Med*. 2017;38(4):e16-47.
 43. Bamber J, Cosgrove D, Dietrich CF, Fromageau J, Bojunga J, Calliada F, et al. EFSUMB guidelines and recommendations on the clinical use of ultrasound elastography. Part 1: basic principles and technology. *Ultraschall Med*. 2013;34(2):169-84.
 44. Barr RG, Ferraioli G, Palmeri ML, Goodman ZD, Garcia-Tsao G, Rubin J, et al. Elastography assessment of liver fibrosis: society of radiologists in ultrasound consensus conference statement. *Radiology*. 2015;276(3):845-61.
 45. Li YY, Wang XM, Zhang YX, Ou GC. Ultrasonic elastography in clinical quantitative assessment of fatty liver. *World J Gastroenterol*. 2010;16(37):4733-7.
 46. Sigrist RM, Liau J, Kaffas AE, Chammas MC, Willmann JK. Ultrasound elastography: review of techniques and clinical applications. *Theranostics*. 2017;7:1303-29.
 47. Thitaikumar A, Ophir J. Effect of lesion boundary conditions on axial strain elastograms: a parametric study. *Ultrasound Med Biol*. 2007;33(9):1463-7.
 48. Ferraioli G, De Silvestri A, Lissandrini R, Maiocchi L, Tinelli C, Filice C, et al. Evaluation of inter-system variability in liver stiffness measurements. *Ultraschall Med*. 2019;40(1):64-75.
 49. Nightingale K. Acoustic Radiation Force Impulse (ARFI) imaging: a review. *Curr Med Imaging Rev*. 2011;7(4):328-39.

50. Dooley MM. Model-based elastography: a survey of approaches to the inverse elasticity problem. *Phys Med Biol.* 2012;57(3):R35-73.
51. Selladurai S, Thittai AK. Strategies to obtain subpitch precision in lateral motion estimation in ultrasound elastography. *IEEE Trans Ultrason Ferroelectr Freq Control.* 2018;65(3):448-56.
52. Luo J, Konofagou EE. Effects of various parameters on lateral displacement estimation in ultrasound elastography. *Ultrasound Med Biol.* 2009;35(8):1352-66.
53. Rao M, Chen Q, Shi H, Varghese T, Madsen EL, Zagzebski JA, et al. Normal and shear strain estimation using beam steering on linear-array transducers. *Ultrasound Med Biol.* 2007;33(1):57-66.